ACCEPTED MANUSCRIPT
AIP Advances
AIP Publishing
This is the author's peer reviewed, accepted manuscript. However, the online version of record will be different from this version once it has been copyedited and typeset.
PLEASE CITE THIS ARTICLE AS DOI: 10.1063/5.0155054

Disentangling the Confounding Spectroscopy of C_1 Molecules: Without Symmetry as a Guide, Everything is Allowed

Michael J. Wilhelm,* Timothy J. Johnson, and Tanya L. Myers
Physical Sciences Division, Pacific Northwest National Laboratory, Richland, WA 99352, USA
* Author to whom correspondence should be addressed. E-mail: michael.wilhelm@pnnl.gov

ABSTRACT
The spectra of C_1 molecules are confounding in that each of the fundamental vibrational modes transform as the exact same irreducible representation (A) and hence each band consists of a seemingly random distribution of a-, b-, and c-type transitions. This is in contrast to higher symmetry molecules for which band types are readily deduced by simple symmetry rules. Herein, we present a method to simulate the convoluted rotational contours in the gas-phase spectra of C_1 molecules by combining existing *ab initio* calculations with Colin Western's PGOPHER rotational contour program. Specifically, *ab initio* calculations in the NWCHEM suite of programs were employed to predict the components of the dipole moment derivatives along the principal axes of the moments of inertia. This information was then input into PGOPHER to model the fundamental band contours as a sum of a-, b-, and c-type transitions. This method was applied to simulate the rotational contour spectra of a series of representative C_1 molecules which were then compared against both *ab initio* stick spectra and experimentally measured broadband IR spectra from the Pacific Northwest National Laboratory infrared gas-phase database. In addition to providing further insight beyond what is revealed in a typical stick spectrum, the simulated contours showed good agreement with the measured spectra.

KEYWORDS
Gas-phase; IR spectra; rotational contour; PGOPHER; C_1 symmetry

ACCEPTED MANUSCRIPT
AIP Advances
AIP Publishing
This is the author's peer reviewed, accepted manuscript. However, the online version of record will be different from this version once it has been copyedited and typeset.
PLEASE CITE THIS ARTICLE AS DOI: 10.1063/5.0155054

INTRODUCTION

Molecular symmetry is a useful predictive tool for the interpretation of molecular spectra, particularly for spectra of gas-phase molecules. Given the point group symmetry of a molecule and the irreducible representations of its individual vibrational modes, it is feasible to partition the associated fundamental transition types as occurring along the three inertial axes and hence exhibiting either an a-, b-, or c-type rotational contour. Conversely, given a spectrum of an unknown gas with distinct band types, it is feasible to use the observed band types (along with calculated frequencies) to interpret the spectrum by assigning the bands to a molecule of a given symmetry and associated functional groups.

Textbooks are filled with numerous examples of predictive tools for highly symmetric molecules [1-4]. However, the overwhelming majority of molecules are actually of C_1 symmetry and are therefore asymmetric tops exhibiting three distinct inertial moments. From a spectroscopic point of view, this obviates the helpful symmetry tools available for interpretation and prediction. For example, even for molecules of limited symmetry (e.g., C_s symmetry), it is feasible to neatly partition the various normal modes into either a/b-type transitions (A') or c-type transitions (A"). This information, along with the fundamental transition frequencies, intensities, and rotational constants (all of which can be deduced via a routine *ab initio* calculation) can be used as input to any of the well-known programs for calculating rotational contours (e.g., PGOPHER) [5] to generate a reasonably accurate simulation of the molecule of interest. Unfortunately, such an analysis cannot be accomplished for C_1 molecules as all of the normal modes correspond to the same irreducible representation (A) and each band can therefore consist of a convoluted mixture of a-, b-, and c-type transitions. For example, as depicted in **Figure 1**, the ν_{20} fundamental mode of 1-butene is predicted to consist of approximately equal parts of an a-, b-, and c-type transition. The distinct band types correspond to projections of the transition dipole moments along the three inertial axes of the molecule, for which c-type bands correspond to transitions along the axis with the largest moment of inertia, a-type bands along the axis with the smallest moment of inertia, and b-type bands correspond to the intermediate case. For C_1 molecules, however, this distribution of transition types is not deducible from symmetry arguments. Fortunately, there is a computationally tractable workaround: Most *ab initio* quantum chemistry programs do in fact routinely calculate the projections of the transition dipole moments (dipole derivatives) along the three principal axes of the molecule. This information is already included as part of the calculation of the absorption intensity, though it is often sequestered in the output file of the calculation. For

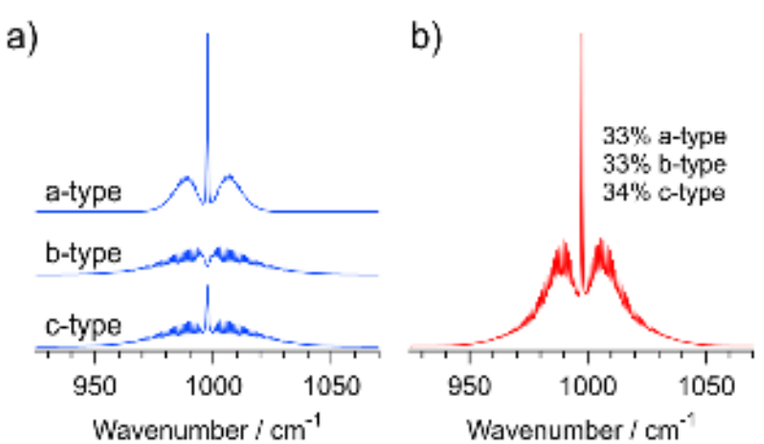

Figure 1. (a) Representative examples of a-, b-, and c-type transitions. (b) Simulated spectrum of the ν_{20} mode of 1-butene constructed using equal parts of the three transition types depicted in (a). The simulations used calculated rotational constants of: A = 0.7615 cm^{-1}, B = 0.1375 cm^{-1}, and C = 0.1342 cm^{-1}.

ACCEPTED MANUSCRIPT
AIP Advances
AIP Publishing
This is the author's peer reviewed, accepted manuscript. However, the online version of record will be different from this version once it has been copyedited and typeset.
PLEASE CITE THIS ARTICLE AS DOI: 10.1063/5.0155054

example, while GAUSSIAN calculates the dipole derivatives, this information is not included in the output unless the command IOP(7/33=1) is included in the route section.[6]

While C_1 molecules are classified in the most challenging molecular point group with respect to their spectra (i.e., the a-, b-, and c-type transitions are all allowed for each vibrational mode), many of the other lower symmetry groups also provide only limited symmetry information regarding the type of rotational contour. For example, for the many C_s molecules, while c-type transitions are allowed for A" vibrational modes, A' modes consist of a seemingly random mixture of a- and b-type bands, the extent of which cannot be deduced from symmetry arguments. A perusal of the character tables quickly reveals that numerous other higher symmetry point groups also exhibit this frustrating limitation and therefore can likewise be better understood using the methods outlined in this paper (i.e., this approach is not limited to C_1 molecules). Nevertheless, such considerations are most relevant to C_1 and C_s molecules due to the predominance of molecules found in these lower symmetry groups.

It is also worth noting that this approach is intended solely for gas-phase (as opposed to condensed-phase) spectra which can exhibit characteristic rotational contours even for relatively poor spectral resolution. Historically, such an analysis was prohibitively cumbersome, as it often required use of complicated custom programs with steep learning curves. Thanks to the availability of open-source and easy to use rotational contour programs, such as Western's PGOPHER program [5], such analysis is now readily accomplished. Further, while there exist many spectral databases devoted to various classes of molecules [7-9], there are always deficiencies and hence there exists a persistent need to model spectra which have not yet been experimentally observed. This is especially true for spectra observed under conditions of reaction (e.g., photolysis, combustion) [10-12]. Using a variety of *ab initio* programs, it is now routine to calculate the fundamental vibrational modes of a molecule of interest and generate a stick spectrum. Stick spectra are useful tools for interpreting vibrational spectra. However, using the exact same calculations needed to generate a stick spectrum, it is now relatively facile to also generate the rotational contours (e.g., using programs such as PGOPHER). As compared to simple stick spectra, rotational contours provide a wealth of additional structural information for assigning spectral bands. Of course, as noted above, such analysis is not trivial for C_1 molecules. Realizing that the overwhelming majority of molecules belong to lower-symmetry groups, this paper reports on a method to aid in vibrational assignment of such gas-phase molecular spectra. Specifically, using *ab initio* quantum chemistry programs in combination with PGOPHER, it is possible to take the relative fraction of intensity predicated along the three principal axes of inertia to simulate the bands' rotational contours as a combination of a-, b- and c-type bands. The method is demonstrated via the simulated rotational contours of a series of representative C_1 molecules, namely propylene oxide, β-pinene, 1-butene, and acetone cyanohydrin which are compared to the experimentally measured broadband IR spectra whose data were obtained from the Pacific Northwest National Laboratory (PNNL) infrared gas-phase database.

MATERIALS and METHODS

A. Experimental details for the gas-phase mid-IR spectra

The experimental data presented in this paper were all recorded as part of the PNNL infrared spectroscopic database. The composite infrared spectra correspond to those of individual pure molecules, with data recorded of the gas when pressure broadened to 760 Torr with N_2(g). The experimental parameters used to acquire and process these data have all been reported previously in the literature [9,13-16]. The data retain the important quality that they are quantitative

ACCEPTED MANUSCRIPT
AIP Advances
AIP Publishing
This is the author's peer reviewed, accepted manuscript. However, the online version of record will be different from this version once it has been copyedited and typeset.
PLEASE CITE THIS ARTICLE AS DOI: 10.1063/5.0155054

on the y-axis and represent a spectroscopic burden of 1 ppm-meter. The other important acquisition parameter, especially in terms of the present study, is the spectroscopic resolution. All of the spectra were all recorded at 0.11 cm^{-1}. Such a resolution is sufficient to resolve nearly all of the pressure broadened lines. For the present study, it also means that the rotational contour profile of all bands are resolved [17,18] and can be used to determine the a-, b, or c-type nature of the contour (or some combination thereof) as described below. The acquired reference spectra from the database include the gas-phase data of ethylene, propylene oxide, β-pinene, 1-butene, and acetone cyanohydrin.

B. *Ab initio* calculations and rotational contour analysis

A series of density functional theory calculations were performed using the NWCHEM suite of programs to model the equilibrium geometries and IR spectra of all molecules considered in this study [19]. All calculations were performed at the B3LYP/6-311++G** level of theory [20-24]. In addition to the global minimum energy molecular geometries, additional calculations were performed for a select sampling of molecules in an effort to preferentially favor higher symmetry structures. In all cases, the higher symmetry geometries were found to exhibit higher zero-point energies (ZPEs) and were shown to correspond to either high energy minima on the potential energy surface (PES) or transition states whose imaginary frequency mode led to the global minimum structure. The deduced harmonic frequencies were globally scaled by a precalculated factor of 0.9679 [25,26]. The output of the calculations, including the rotational constants, the harmonic frequencies of the fundamental vibrational modes, the point group symmetry of the optimized structure, the irreducible representations of the fundamental modes, and the projections of the transition dipole moments (for each fundamental mode) onto the three principal axes, were used as inputs for simulating the rotational contour using Colin Western's PGOPHER program [5]. All contours were simulated as asymmetric tops using a temperature of 298.15 K, a J_{max} of 100, and each transition was broadened using a 2 cm^{-1} wide Lorentzian line shape.

RESULTS and ANALYSIS

A. A high-symmetry example: Ethylene

Before considering examples of C_1 molecules, it is instructive to examine a well-behaved case where molecular symmetry is advantageous. In particular, the highly symmetric molecule, ethylene, the simplest alkene (CH_2CH_2, D_{2h} symmetry) is considered. Similar to C_{2v} molecules, D_{2h} molecules retain the useful symmetry property that all of their IR-active modes yield pure transition band type character (i.e., a-, b-, or c-). This can be inferred from the fact that each of the three IR-active irreducible representations in the D_{2h} table are uniquely aligned along only one of the three projections of the transition dipole moment. Specifically, the b_{1u} modes are allowed via transitions along the z-axis, the b_{2u} modes along the y-axis, and the b_{3u} modes along the x-axis. Given the convention that a-type (c-type) transitions correspond to changes along the axis with the smallest (largest) moment of inertia and b-type transitions correspond to the intermediate case, knowing the irreducible representations of the IR-active modes accurately reveals the expected transition band type for each fundamental mode [14,27-29]. From this it follows that the fundamental IR spectrum of ethylene should consist of twelve fundamental vibrational modes, only five of which are IR-active with one c-type band (b_{1u}), two b-type bands (b_{2u}), and two a-type bands (b_{3u}).

As a test of this assertion, *ab initio* calculations were run in order to model the vibrational properties of ground state ethylene (i.e., the geometry was optimized and the harmonic fundamental vibrational modes were calculated). In addition to predicted transition frequencies and absorption intensities, the calculations also yielded an estimate of the three equilibrium

ACCEPTED MANUSCRIPT
AIP Advances
AIP Publishing
This is the author's peer reviewed, accepted manuscript. However, the online version of record will be different from this version once it has been copyedited and typeset.
PLEASE CITE THIS ARTICLE AS DOI: 10.1063/5.0155054

rotational constants, the eigenvalues of the moment of inertia matrix, and the projections of the transition dipole moments (dipole derivatives) along the three principal axes for each normal mode. The eigenvalues of the moment of inertia matrix were used to assign the three principal axes (a-, b-, and c-). It is worth noting that the NWCHEM suite of programs appears to use the convention of ordering the inertial axes using the IIIℓ representation (i.e., x→b, y→a, z→c) [28].

Ethylene has calculated equilibrium rotational constants of A=4.910 cm^{-1}, B=1.007 cm^{-1}, and C=0.835 cm^{-1}, which yields an asymmetry parameter (κ=[2B-A-C]/[A-C]) of κ = -0.916, suggesting that it is a near-prolate symmetric top. The calculated transition frequencies, transition moment projections, rotational constants, and irreducible representations of the five IR-active modes of ethylene were all used as inputs for the PGOPHER program and a simulated rotational contour spectrum was generated. **Figure 2** depicts a comparison of the measured gas-phase IR spectrum (black trace), simulated rotational contour spectrum (red trace), and the *ab initio* calculated stick spectrum (blue lines) for the fundamental modes of ethylene. Additionally, the projections of the calculated transition dipole moments (each individually normalized to one) along the three inertial axes are depicted in a grayscale color matrix near the top of the figure. Note that the rows of the matrix correspond to the a-, b-, or c-type character, whereas each column represents the intensity distribution for each fundamental mode. Consistent with expectation based on the point group symmetry, the transition dipole moments for each of the IR-active modes is shown to be perfectly aligned along only one of the three inertial axes (and appears black in the corresponding box).

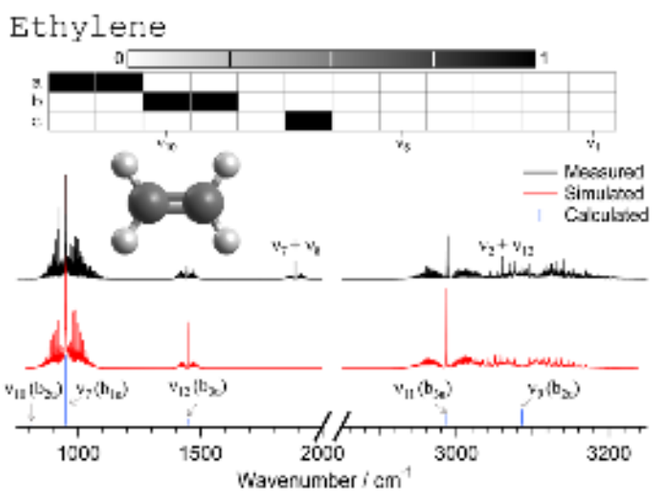

Figure 2. Comparison of the measured (black trace) and simulated rotational contour (red trace) gas-phase IR spectrum of ethylene. The simulated spectrum was deduced using *ab initio* calculated stick spectra frequencies (blue lines). The grayscale color matrix near the top depicts the projections of the transition dipole moments for each of the 12 fundamental vibrational modes onto the three principal axes of the molecule.

As shown in **Figure 2**, the simulated rotational contour (red trace) is in excellent agreement with the experimental gas-phase spectrum (black trace). It is emphasized that no attempt was made to improve the simulated contour to better match the experimental data (e.g., variation in intensities, rotational constants, etc.). Aside from applying a standard frequency scaling factor for anharmonic frequency correction, the rotational contour shown is based solely upon the raw output of the *ab initio* calculation. Perhaps the most obvious difference is the absence of the $\nu_7+\nu_8$ combination band near 1890 cm^{-1} [30]. Also, though less obvious, is the absence of the less intense $\nu_2+\nu_{12}$ combination band near 3080 cm^{-1} [30]. This can be understood as the simulated contours include only the fundamental vibrational modes. Consequently, especially in the C_1

ACCEPTED MANUSCRIPT
AIP Advances
AIP Publishing
This is the author's peer reviewed, accepted manuscript. However, the online version of record will be different from this version once it has been copyedited and typeset.
PLEASE CITE THIS ARTICLE AS DOI: 10.1063/5.0155054

examples to be presented below, any bands present in the measured spectra but absent from the simulated contours likely stem from combination or overtone bands. While ethylene has five IR-active fundamental modes, the simulation seems to show only four distinct ro-vibrational bands. Closer inspection of the *ab initio* blue stick spectrum shows that there were indeed five IR-active modes predicted in the calculation. Nevertheless, the ν_{10} CH_2-rocking mode at 826 cm^{-1} is comparatively weak relative to the other four IR-active modes. While the weak ν_{10} mode was included in the rotational contour, it does not contribute significantly to the resulting spectrum. As expected, the spectrum of ethylene is indeed shown to be composed of a single c-type band (ν_7) near 1000 cm^{-1}; two b-type bands, the weak ν_{10} transition near 800 cm^{-1} and the ν_9 transition near 3100 cm^{-1}; and two a-type transitions, the ν_{12} and ν_{11} transitions near 1500 and 3000 cm^{-1}, respectively. This agreement with measurement lends credence to the approach of using *ab initio* calculations as inputs for `PGOPHER`-deduced rotational contours in the analysis of the more complex examples of molecules exhibiting C_1 symmetry. Moreover, this example nicely highlights the utility of expanding simple stick spectra into rotational contours for a clearer comparison against experimental gas-phase spectra.

B. Low-symmetry examples: C_1 molecules

In the following examples several molecules exhibiting C_1 symmetry are considered. The simulated rotational contours of these molecules represent the unmodified results of *ab initio* calculations. In other words, the calculated parameters (e.g., the ratios of the transition dipole moment projections) were not refined to better match the experimental spectra. The only exception is that the prescribed frequency scaling factor for `B3LYP/6-311++G**` calculations (i.e., 0.9679) was globally applied to all simulated spectra and additional (local) frequency scaling was applied to each spectral range shown [25,26]. Aside from this factor, the absorption intensity and band type ratios all represent the raw output values of the *ab initio* calculations. As in the ethylene case above, the calculations include only the fundamental vibrational modes of the molecules under study (i.e., hot bands, combination bands, or difference bands were not included). Finally, in all of the examples presented below, the deduced symmetry of the calculated optimized structure was resolutely deduced as C_1. In a few of the examples, however, it is clear that additional bond rotations could result in the molecule exhibiting C_s symmetry (albeit at a higher energy). Each of these examples originated from achiral molecules, identified by the lack of a chiral center. These examples further highlight the utility of the present approach and will be considered separately.

i.) Chiral C_1 molecules

In this section, we consider example chiral molecules, which necessarily exhibit C_1 symmetry. Specifically, we examine the spectra of propylene oxide and β-pinene.

(1) *Propylene oxide*

Propylene oxide (C_3H_6O) is a chiral epoxide and has recently been experimentally observed in the interstellar medium [31]. It has 24 fundamental vibrational modes and, by virtue of the fact that it has C_1 symmetry, all vibrational modes are IR-active. However, while symmetry allows all the transitions, this does not imply that each of the vibrational modes will have sufficient oscillator strength to be experimentally observed. The calculated equilibrium rotational constants are A = 0.605 cm^{-1}, B = 0.221 cm^{-1}, and C = 0.197 cm^{-1}, approximately an order of magnitude smaller than those of ethylene. Nevertheless, this yields an asymmetry parameter of κ = -0.882 and identifies propylene oxide as a near-prolate symmetric top.

ACCEPTED MANUSCRIPT
AIP Advances
AIP Publishing
This is the author's peer reviewed, accepted manuscript. However, the online version of record will be different from this version once it has been copyedited and typeset.
PLEASE CITE THIS ARTICLE AS DOI: 10.1063/5.0155054

Figure 3 depicts a comparison of the measured gas-phase IR spectrum (black trace), simulated rotational contour spectrum (red trace), and the *ab initio* calculated stick spectrum (blue lines) for propylene oxide. Likewise, the grayscale-colored matrix represents the (individually normalized) transition moment projections onto the three principal axes for each normal mode. Given that all of the fundamental modes (which have been listed on the side of the matrix in steps of 5) share the same irreducible representation (A), they have been ordered such that the first mode (ν_1) corresponds to the highest wavenumber transition (3060 cm^{-1}), down to the last mode (ν_{24}) which corresponds to the lowest wavenumber fundamental (212 cm^{-1}). As distinct from the ethylene case above (**Figure 2**), the transition moment projections for propylene oxide are uniquely distributed along the three principal axes and therefore tend to appear as a near-homogeneous mixture. While there are a few cases in which the transition is predominantly aligned along one of the three axes (e.g., ν_6 and ν_{10} along the a-axis, ν_4 and ν_9 along the b-axis, and ν_8 and ν_{11} along the c-axis), the majority of the transitions are randomly projected on all three. When viewed across a broad spectral range, there is excellent agreement between the measured and simulated rotational contour spectrum of propylene oxide. However, the lower energy portion of the spectrum (i.e., 600-1700 cm^{-1}) appears to show slightly better agreement compared to the higher energy portion (i.e., 2600-3200 cm^{-1}) which corresponds to the C-H stretching modes. This can be ascribed to greater inaccuracies in calculated C-H stretch frequencies compared to C-C or C-O modes, due to the fact that higher energy modes (such as C-H stretches) are more sensitive to effects of anharmonicity [32].

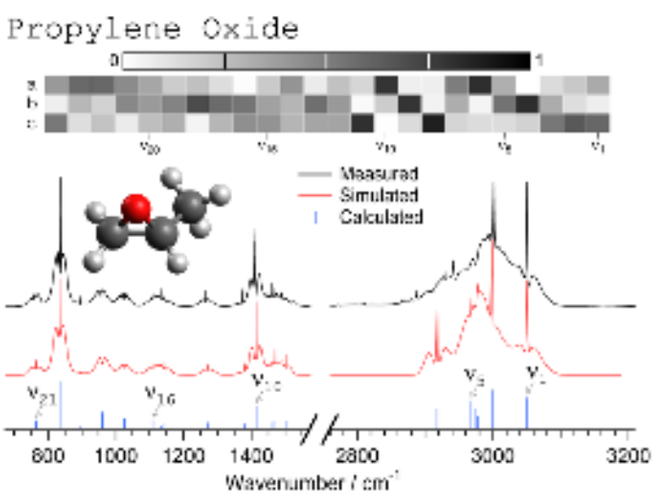

Figure 3. Comparison of the measured (black trace) and rotational contour simulated (red trace) gas-phase IR spectrum of propylene oxide. The simulated spectrum was deduced using *ab initio* calculated stick spectra frequencies (blue lines). The grayscale color matrix near the top depicts the projections of the transition dipole moments for each of the 24 fundamental vibrational modes onto the three principal axes of the molecule.

(2) *β-Pinene*

β-pinene ($C_{10}H_{16}$) is a chiral bicyclic unsaturated terpene found in the leaves of coniferous trees [33]. With 26 atoms it has 72 fundamental modes and, like all C_1 molecules, each of the modes is IR-active. The calculated rotational constants of β-pinene are A = 0.0633 cm^{-1}, B = 0.0427 cm^{-1}, and C = 0.0381 cm^{-1}, two orders-of-magnitude smaller than those of ethylene. This indicates that the various ro-vibrational energy levels of β-pinene will be more closely spaced than in the prior two examples and hence the resulting bands will be narrower. Similar to the two prior cases, β-pinene has an asymmetry parameter of κ = -0.635 and is also a near-prolate symmetric top.

ACCEPTED MANUSCRIPT
AIP Advances
AIP Publishing
This is the author's peer reviewed, accepted manuscript. However, the online version of record will be different from this version once it has been copyedited and typeset.
PLEASE CITE THIS ARTICLE AS DOI: 10.1063/5.0155054

Figure 4 plots the measured gas-phase IR spectrum (black trace), simulated rotational contour spectrum (red trace), and the *ab initio* calculated stick spectrum (blue lines) for β-pinene. Given the comparatively small rotational constants, it is perhaps reasonable to initially speculate that the rotational contours for each of the ro-vibrational bands of β-pinene will simply collapse into an unresolvable feature, better described by a simple Lorentzian / Gaussian line shape. As observed in **Figure 4,** however, aspects of the rotational contour still persist in the measured spectrum (particularly the Q-branches) and therefore validate the utility of rotational contours for analysis. As was the case for propylene oxide, the majority of modes exhibit a mixture of projections onto all three axes. This is consistent with C_1 symmetry and the lack of symmetry-based constraints to otherwise align the transitions. Similar to propylene oxide (**Figure 3**), there is clearly better agreement between the measured and simulated spectra in the lower energy range (i.e., 700-1800 cm^{-1}) compared to the higher energy range (i.e., 2850-3150 cm^{-1}) which shows the most significant deviations from the measured spectrum. Nevertheless, there are also notable differences in the low energy range. For example, there is what appears to be a combination band near 1750 cm^{-1} which is absent in the simulation since these contours only include the fundamental vibrational modes. Likewise, the ν_{53} band (a dominant c-type band) near 850 cm^{-1} appears to be shifted to lower energy as compared to the experimental spectrum. Further, the ν_{17} band near 1650 cm^{-1}, which is predicted to have approximately equal parts a- and b-type character, appears to have greater a-type character than what is observed in the measured spectrum. Despite these relatively minor differences, **Figure 4** shows that there is very good agreement between the measured and simulated spectra.

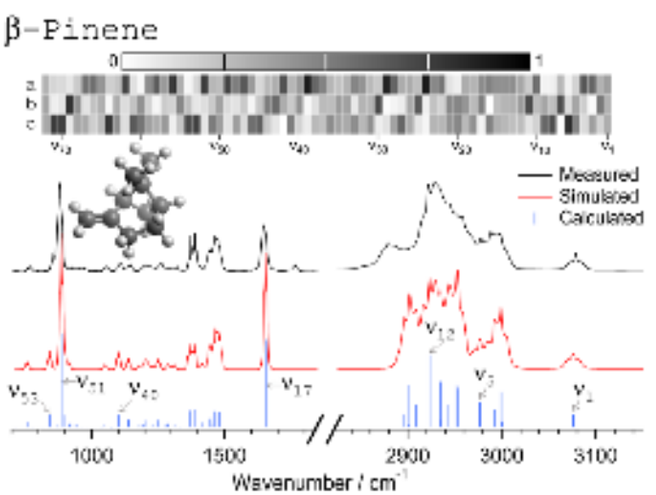

Figure 4. Comparison of the measured (black trace) and simulated rotational contour (red trace) gas-phase IR spectrum of β-pinene. The simulated spectrum was deduced using *ab initio* calculated stick spectra frequencies (blue lines). The grayscale color matrix near the top depicts the projections of the transition dipole moments for each of the 72 fundamental vibrational modes onto the three principal axes of the molecule. Vibrational bands greater than ν_{57} all appear below 700 cm^{-1} and are not depicted in spectra.

ii.) Achiral C_1 molecules: Near-C_s molecules

As distinct from the examples above, the molecules considered in this section are all achiral (i.e., not chiral). Specifically, these molecules do not possess chiral centers and therefore exhibit configurations that can be superimposed on their mirror images. Each of the molecules examined nevertheless exhibited *ab initio* calculated structures of C_1 symmetry. Close examination of the resulting optimized structures reveals, however, that simple rotation about one or more of the bonds could instead give rise to higher energy configurations exhibiting C_s symmetry. In these

ACCEPTED MANUSCRIPT
AIP Advances
AIP Publishing
This is the author's peer reviewed, accepted manuscript. However, the online version of record will be different from this version once it has been copyedited and typeset.
PLEASE CITE THIS ARTICLE AS DOI: 10.1063/5.0155054

examples, through direct comparison with the experimentally measured spectra, we examine which representation (i.e., C_1 vs. C_s) yields the best description of the system.

(1) *1-Butene*

In this section, the spectrum of 1-butene ($C_3H_5CH_3$) is investigated. Similar to the previous examples, 1-butene is a near-prolate symmetric top with rotational constants comparable in magnitude to propylene oxide (**Figure 3**). *Ab initio* calculations predict an optimized geometry corresponding to C_1 symmetry. However, closer examination of the resulting structure suggests that a simple torsional motion along the central C-C bond could in fact increase the point group symmetry to C_s. Additional calculations were performed with the aim of optimizing the geometry to the higher symmetry structure to investigate if this would better reproduce the measured spectrum. Consistent with expectation, the C_s geometry was shown to have a ZPE approximately 2 kcal/mole higher than the corresponding C_1 geometry. More importantly, the optimized C_s geometry was shown to correspond to a transition state rather than a local minimum. The associated imaginary frequency mode was shown to be a torsional motion leading back to the global minimum C_1 geometry. As a result, despite the energetic proximity to a higher symmetry geometry, the ground state of 1-butene appears to be best described as a C_1 molecule. This behavior was also observed for structurally similar molecules, allyl bromide and allyl alcohol (data not shown).

Comparisons of the measured gas-phase IR spectrum (black trace), simulated rotational contour spectrum (red trace), and the *ab initio* calculated stick spectrum (blue lines) for 1-butene are depicted in **Figure 5**. As in the examples above, the simulated rotational contour spectrum agrees well with the experimentally measured spectrum. This provides additional credence for the assignment of C_1 symmetry for 1-butene. It is also of interest to consider the observed pattern of the projections of the transition dipole moments. Given how close the structure was to exhibiting C_s symmetry, it is reasonable to expect that the spectrum could likewise exhibit a near-C_s rotational pattern. In particular, the vibrational modes of C_s molecules transform as irreducible representations of either A' (corresponding to a mixture of a- and b-type transitions) or A" (c-type transitions). The transition dipole moment projections of the A' modes would be distributed along the a- and b-axes, with no component on the c-axis. Conversely, all of the A" modes would be

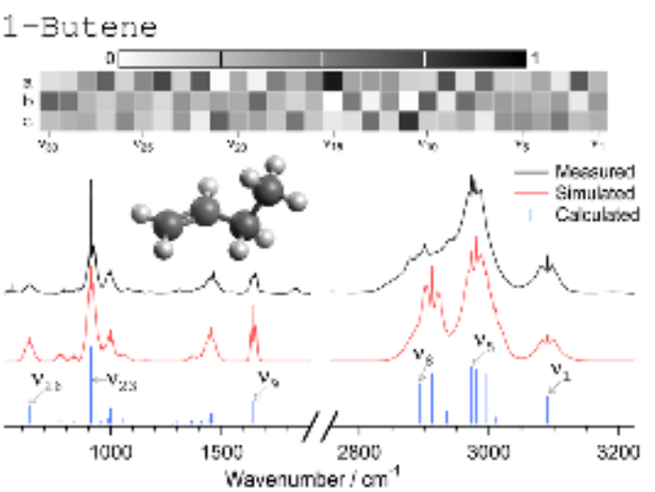

Figure 5. Comparison of the measured (black trace) and simulated rotational contour (red trace) gas-phase IR spectrum of 1-butene. The simulated spectrum was deduced using *ab initio* calculated stick spectra frequencies

ACCEPTED MANUSCRIPT
AIP Advances
AIP Publishing
This is the author's peer reviewed, accepted manuscript. However, the online version of record will be different from this version once it has been copyedited and typeset.
PLEASE CITE THIS ARTICLE AS DOI: 10.1063/5.0155054

(blue lines). The grayscale color matrix near the top depicts the projections of the transition dipole moments for each of the 30 fundamental vibrational modes onto the three principal axes of the molecule.

projected solely along the c-axis. Similar to the ethylene example above (**Figure 2**), this would correspond to white blocks in the a and b rows (i.e., exactly zero) and a black block in the c row (i.e., exactly one). Further, examination of the *ab initio* calculation for the predicted C_s transition state geometry reveals that 10 of the 30 fundamental modes are described as having irreducible representations of A" and should therefore exhibit transition dipole moment projections solely along the c-axis. With rare exception, most of the transition intensity is partitioned among the a- and b-axes. When coupled with the overall better agreement between the C_1 simulation and the experimental spectrum, this further substantiates the assignment of C_1 geometry for 1-butene.

(2) *Acetone Cyanohydrin*

Acetone cyanohydrin (C_4H_7ON) is another example of an achiral molecule exhibiting C_1 symmetry. Similar to 1-butene examined above, *ab initio* calculations predict a global minimum configuration of acetone cyanohydrin with C_1 symmetry. However, unlike 1-butene, our calculations also identified a separate local minimum on the PES exhibiting C_s symmetry (i.e., not a transition state). The deduced C_s local minimum of acetone cyanohydrin is predicted to be ca. 2.16 kcal/mole above the ZPE of the C_1 global minimum. Based upon a Boltzmann distribution, such an energy difference suggests that a room temperature population of acetone cyanohydrin would overwhelmingly consists of the C_1 conformer (C_1 : C_s = 38.3 : 1, or roughly 98% C_1). Beyond the possibility of energetically accessible conformers, this example also serves as a cautionary tale about calculating the wrong geometry and the associated inaccuracies in the simulated spectrum. Simulated rotational contours for both the C_1 and C_s geometries were prepared for comparison against the experimentally measured spectrum in **Figure 6**.

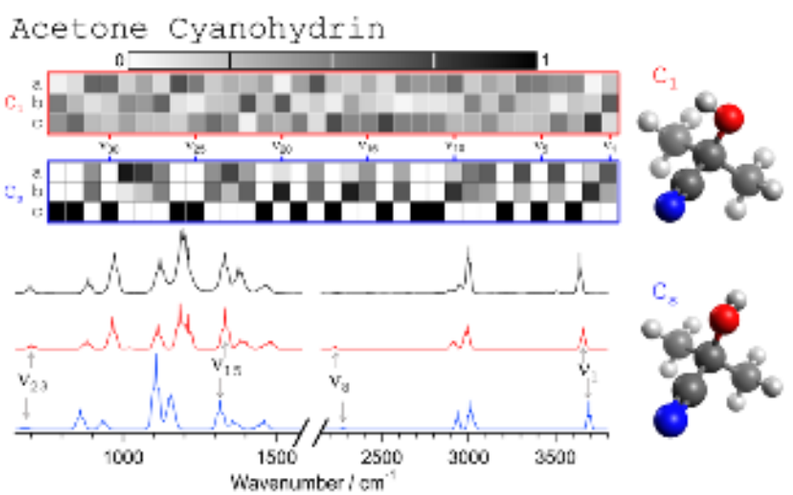

Figure 6. Comparison of the measured (black trace) and rotational contour simulations (C_1 geometry, red trace and C_s geometry, blue trace) for the gas-phase IR spectrum of acetone cyanohydrin. The grayscale color matrix near the top depict the projections of the transition dipole moments for each of the 33 fundamental vibrational modes onto the three principal axes of the molecule deduced for C_1 (top, red outline) and C_s (bottom, blue outline) geometry.

As should be expected, the C_1 and C_s simulated spectra are clearly different. In addition to variations in the predicted transition frequencies, the projections of the transition dipoles onto the principal axes reveal that the intensity profiles are unique. Note that, for ease of comparison, the numbering of the fundamental vibrational modes (tabulated between the two matrices in

ACCEPTED MANUSCRIPT
AIP Advances
AIP Publishing
This is the author's peer reviewed, accepted manuscript. However, the online version of record will be different from this version once it has been copyedited and typeset.
PLEASE CITE THIS ARTICLE AS DOI: 10.1063/5.0155054

increments of 5) was ordered in decreasing wavenumbers for both the C_1 and C_s systems (i.e., ν_1 represents the highest wavenumber mode and ν_{33} the lowest wavenumber mode). Despite their similar overall geometries, the intensity profile of the C_1 molecule is characteristically distinct compared to the C_s molecule. Specifically, whereas the intensity projections in the C_s molecule are strictly aligned either along the c-axis or a mix of the a-/b-axis, the projections in the C_1 molecule appear randomly distributed (i.e., nearly homogeneous) along all three axes, which is consistent with the other C_1 examples presented above.

Overall, the C_1 geometry appears to be more consistent with the experimental spectrum, particularly in the low energy region (ca. 700-1500 cm^{-1}). For example, while the ν_{22} (855 cm^{-1}) and ν_{20} (940 cm^{-1}) modes appear to exhibit similar mixtures of band types in both the C_1 and C_s contours, the predicted intensities in the C_1 contour are more accurate. Likewise, the frequency distribution and intensities of the transitions in the 1100-1300 cm^{-1} range show better agreement in the C_1 contour. Interestingly, while the predicted C-H stretching modes appear similar in both the C_1 and C_s contours, neither matches well with the experimental. As noted above, this likely stems from effects of anharmonicity and/or the influence of combination bands. Finally, it is of interest to consider the ν_1 O-H stretch band near 3700 cm^{-1}, as the relative orientation of this functional group is at the heart of the two distinct geometries. Here, the C_1 simulation seems to exhibit better agreement with the measured spectrum as it possess significant c-type band character (i.e., 43% c-type, 52% b-type, and 6% a-type). Conversely, the O-H stretch in the C_s simulation is an A" mode and therefore contains no c-type character but is instead composed solely of a-type (65%) and b-type (35%) character. Consequently, here too we find that the experimental spectrum is most consistent with an assignment of C_1 symmetry.

DISCUSSION

In this study, we have employed a combination of *ab initio* calculations in the NWCHEM suite of programs and Western's PGOPHER rotational contour program to simulate the IR rotational contour spectra of a series of molecules exhibiting C_1 symmetry. The high symmetry example of ethylene (D_{2h}) was used as proof-of-principle to establish the protocols. The more confounding cases of C_1 molecules, including both chiral and achiral systems were then examined. Besides highlighting the utility of rotational contour simulation programs, the results were also compared to *ab initio* stick spectra, which are routinely used in spectroscopy studies as they offer a convenient representation of the predicted frequency and relative intensity of a vibrational mode. It is worth noting that the same *ab initio* calculations required to produce a stick spectrum provide all the necessary information to generate a rotational contour. As demonstrated in this paper, rotational contours are easily calculated using established open-source programs (such as PGOPHER) and yield greater insight, particularly for molecules exhibiting C_1 symmetry.

For studies focused on the spectra of pure samples, it is often sufficient to only know the predicted frequency and intensity of the various fundamental modes. Specifically, provided most of the fundamental modes can be measured, it is feasible to make a convincing spectral assignment using only a stick spectrum [14,29,34-36]. Unfortunately, there are numerous scenarios for which it is not always possible to obtain pure samples. For example, transient or trace species, such as high energy geometric isomers (e.g., HNC, H_2C=C:) [37,38] and reactive species like radicals (e.g., HCCO) [39,40] need to be photolytically or thermally produced as their lifetimes are short [10,32,41,42]. The problem then arises that in addition to the species of interest, such spectra typically contain overlapping contributions from the parent precursor as well as a variety of subsequent reaction products. The resulting spectra tend to be a convolution of overlapping bands which offer only a limited spectral window from which perhaps one or two bands of the

ACCEPTED MANUSCRIPT
AIP Advances
AIP Publishing
This is the author's peer reviewed, accepted manuscript. However, the online version of record will be different from this version once it has been copyedited and typeset.
PLEASE CITE THIS ARTICLE AS DOI: 10.1063/5.0155054

target species can be resolved. While stick spectra offer a sense of where to look for new bands, a rotational contour nicely reveals how the new bands should appear and can therefore greatly aid in spectral assignment.

A further limitation of using stick spectra for assignments is that care must be exercised as stick spectra can lead to ambiguous interpretation of relative intensities. Depending upon whether a given transition possess a strong Q-branch (i.e., a-type or c-type bands) can influence the apparent intensity of that band. For example, consider the ν_9 and ν_{11} modes of ethylene (**Figure 2**). Based upon the *ab initio* stick spectrum (blue trace), if nothing were known about the band types, it would be reasonable to speculate that the ν_9 mode should be ca. 1.5 times more intense than the ν_{11} mode. In reality, however, due to the presence of the strong Q-branch in the ν_{11} mode (a-type band), its maximum intensity is actually more than four times greater than that of the ν_9 mode (b-type band). Disentangling this spectral scenario can be accomplished by making use of rotational contours. We note, however, while rotational contours can provide excellent agreement with experimental spectra, they are not without limitation. The quality of the rotational contour spectrum is ultimately linked to the accuracy of the input parameters obtained from the preceding *ab initio* calculation. As noted in the case of 1-butene (**Figure 5**) and acetone cyanohydrin (**Figure 6**), if the symmetry of the molecule is incorrectly assigned, the predicted spectrum will deviate from the measurement.

Finally, it is important to recall that (at least for the cases examined above) the low energy region of the simulated contours tended to be in better agreement with the experimentally measured spectra. As noted earlier, this may stem from inaccuracies associated with calculating C-H stretch frequencies, as well as whether or not combination-bands etc. are considered. In general, C-H stretching modes tend to be more significantly influenced by anharmonicities in the vibrational potential [3,43]. For the examples considered here, we simply applied an *ad hoc* global frequency scaling factor to approximate the influence of anharmonicity. A more refined approach would require more accurate (and therefore more expensive) *ab initio* calculations which explicitly includes higher order terms of the potential surface and therefore a more quantitative assessment of anharmonic effects. Such calculations also tend to permit assessment of the various combination-bands etc., which would likewise provide a more accurate model of the higher energy region of the spectrum.

SUMMARY

Molecules that contain varying degrees of symmetry have their spectroscopic analysis (including their vibrational spectra) simplified via the use of group theory. This is particularly the case for molecules with high symmetry. Fundamentally, this arises because the symmetry operators commute with the Hamiltonian. However, the vast majority of molecules belong to lower-symmetry groups such as C_s or C_1, where the guiding rules of symmetry are not as useful and it is therefore expedient to find alternative methods to help interpret a spectrum. This paper reports on a method that yields better insight into vibrational spectral assignments. Specifically, we have demonstrated that using the results of *ab initio* programs (e.g., NWCHEM) in combination with the rotational contour program PGOPHER, it is possible to use the relative fraction of intensity along the three principal axes of inertia to predict the bands' rotational contours as a combination of a-, b- and c-type bands. Convolution of the rotational contour with the energy eigenvalue (stick) spectrum was demonstrated to improve the vibrational analysis of a series of representative gas-phase spectra from molecules of C_1 symmetry.

ACCEPTED MANUSCRIPT
AIP Advances
AIP Publishing
This is the author's peer reviewed, accepted manuscript. However, the online version of record will be different from this version once it has been copyedited and typeset.
PLEASE CITE THIS ARTICLE AS DOI: 10.1063/5.0155054

ACKNOWLEDGEMENTS
This work was supported by the Department of Defense's Strategic Environmental Research and Development Program (SERDP), environmental remediation project ER21-C1-1135 and we thank our sponsors for their support. PNNL is operated for the U.S. Department of Energy by the Battelle Memorial Institute under contract DE-AC06-76RLO 1830.

DATA AVAILABILITY STATEMENT
The data that support the findings of this study are available from the corresponding author upon reasonable request.

AUTHOR INFORMATION
ORCID IDs
- Michael J. Wilhelm: https://orcid.org/**0000-0002-4634-9561**
- Timothy J. Johnson: https://orcid.org/**0000-0001-9514-6288**
- Tanya L. Myers: https://orcid.org/**0000-0001-8995-7033**

REFERENCES
1. G.M. Barrow, Introduction to Molecular Spectroscopy, McGraw Hill, 1962.
2. J.I. Steinfeld, Molecules and Radiation: An Introduction to Modern Molecular Spectroscopy, 2nd edition, Dover Publications, 2005.
3. G. Herzberg, Spectra of Diatomic Molecules, Van Nostrand, 1950.
4. P.F. Bernath, Spectra of Atoms and Molecules, Oxford University Press, 2005.
5. C.M. Western, PGOPHER: A program for simulation rotational, vibrational, and electronic spectra, J. Quant. Spectrosc. Radiat. Transf. 186 (2017) 221-242. https://doi.org/10.1016/j.jqsrt.2016.04.010.
6. M. J. Frisch, G. W. Trucks, H. B. Schlegel, G. E. Scuseria, M. A. Robb, J. R. Cheeseman, G. Scalmani, V. Barone, G. A. Petersson, H. Nakatsuji et al., Gaussian 16, Revision C.01. Gaussian, Inc., Wallingford CT, 2016.
7. I.E. Gordon, L.S. Rothman, R.J. Hargreaves, R. Hashemi, E.V. Karlovets, F.M. Skinner, E.K. Conway, C. Hill, R.V. Kochanov, Y. Tan, The HITRAN2020 molecular spectroscopic database, J. Quant. Spectrosc. Radiat. Transf. 277 (2022) 107949. https://doi.org/10.1016/j.jqsrt.2021.107949.
8. T.J. Baker, R.G. Tonkyn, C.J. Thompason, M.K. Dunlap, P.G. Koster van Gross, N.A. Thakur, M.J. Wilhelm, T.L. Myers, T.J. Johnson, An infrared spectral database for gas-phase quantitation of volatile per- and polyfluoroalkyl substances (PFAS), J. Quant. Spectrosc. Radiat. Transf. 295 (2023) 108420. https://doi.org/10.1016/j.jqsrt.2022.108420.
9. S.W. Sharpe, T. J. Johnson, R.L. Sams, P.M. Chu, G.C. Rhoderick, P.A. Johnson, Gas-Phase Databases for Quantitative Infrared Spectroscopy, Appl. Spectrosc. 58 (2004) 1452-1461. DOI: 10.1366/0003702042641281.
10. K.D. Hughey, R.G. Tonkyn, W.W. Harper, V.L. Young, T.L. Myers, T.J. Johnson, Preliminary studies of UV photolysis of gas-phase CH_3I in air: Time-resolved infrared identification of methanol and formaldehyde products, Chem. Phys. Lett. 768 (2021) 138403. https://doi.org/10.1016/j.cplett.2021.138403.
11. C.A. Banach, A.M. Bradley, R.G. Tonkyn, O.N. Williams, J. Chong, D.R. Weise, T.L. Myers, T.J. Johnson, Dynamic infrared gas analysis from longleaf pine fuel beds burned in a wind tunnel: observation of phenol in pyrolysis and combustion phases, Atmos. Meas. Tech. 14 (2021) 2359-2376. https://doi.org/10.5194/amt-14-2359-2021.
12. N.S. Scharko, A.M. Oeck, T.L. Myers, R.G.Tonkyn, C.A. Banach. S.P. Baker, E.N. Lincoln, J. Chong B.M. Corcoran, G.M. Burke, R.D. Ottmar, J.C. Restaino, D.R. Weise, T.J. Johnson, Gas-phase pyrolysis products emitted by prescribed fires in pine forests with a shrub understory in the southeastern United States, Atmos. Chem. Phys. 19 (2019) 9681-9698. https://doi.org/10.5194/acp-19-9681-2019.
13. S.W. Sharpe, R.L. Sams, T.J. Johnson, P.M. Chu, G.C. Rhoderick, F.R. Guenther, Creation of 0.10 cm^{-1} Resolution, Quantitative, Infrared Spectral Libraries for Gas Sampling, Proc. SPIE 4577 (2002) 457730. https://doi.org/10.1117/12.455730.
14. R. Lindenmaier, S.D. Williams, R.L. Sams, T.J. Johnson, Quantitative Infrared Absorption Spectra and Vibrational Assignments of Crotonaldehyde and Methyl Vinyl Ketone Using Gas-Phase Mid-Infrared, Far-Infrared, and Liquid Raman Spectra: *s-cis* vs *s-trans* Composition Confirmed via Temperature Studies and ab Initio Methods, J. Phys. Chem. A 121 (2017) 1195-1212. https://doi.org/10.1021/acs.jpca.6b10872.

ACCEPTED MANUSCRIPT
AIP Advances
AIP Publishing
This is the author's peer reviewed, accepted manuscript. However, the online version of record will be different from this version once it has been copyedited and typeset.
PLEASE CITE THIS ARTICLE AS DOI: 10.1063/5.0155054

15. T.J. Johnson, K.D. Hughey, T.A. Blake, S.W. Sharpe, T.L. Myers, R.L. Sams, Confirmation of PNNL Quantitative Infrared Cross-Sections for Isobutane, J. Phys. Chem. A 125(17) (2021) 3793-3801. https://doi.org/10.1021/acs.jpca.1c01933.
16. R.V. Kochanov, I.E. Gordon, L.S. Rothman, K.P. Shine, S.W. Sharpe, T.J. Johnson, T.J. Wallington, J.J. Harrison, P.F. Bernath, M. Birk, G. Wagner, K. Le Bris, I. Bravo, C. Hill, Infrared Absorption Cross-Sections in HITRAN2016 and Beyond: Expansion for Climate, Environment, and Atmospheric Applications. J. Quant. Spectrosc. Radiat. Transf. 230 (2019) 172-221. https://doi.org/10.1016/j.jqsrt.2019.04.001.
17. C.S. Brauer, T.A. Blake, A.B. Guenther, S.W. Sharpe, R.L. Sams, T.J. Johnson, Quantitative Infrared Absorption Cross-Sections of Isoprene for Atmospheric Measurements, Atmos. Meas. Tech. 7 (2014) 3839-3847. https://doi.org/10.5194/amt-7-3839-2014.
18. S.D. Williams, T.J. Johnson, S.W. Sharpe, V. Yavelak, R.P. Oates, C.S. Brauer, Quantitative Vapor-Phase IR Intensities and DFT Computations to Predict Absolute IR Spectra Based on Molecular Structure: I. Alkanes, J. Quant. Spectrosc. Radiat. Transf. 129 (2013) 298-307. https://doi.org/10.1016/j.jqsrt.2013.07.005.
19. E. Apra, E.J. Bylaska, W.A. de Jong, N. Govind, K. Kowalski, T.P. Straatsma, M. Valiev, H.J.J. van Dam, Y. Alexeev, J. Anchell et al., NWChem: Past, present, and future, J. Chem. Phys. 152 (2020) 184102. https://doi.org/10.1063/5.0004997.
20. A.D. Becke, A new mixing of Hartree–Fock and local density-functional theories, J. Chem. Phys. 98(2) (1993) 1372-1377. https://doi.org/10.1063/1.464304.
21. C.T. Lee, W.T. Yang, R.G. Parr, Development of the Colle-Salvetti Correlation-Energy Formula into a Functional of the Electron Density, Phys. Rev. B 37(2) 1988 785-789. https://doi.org/10.1103/PhysRevB.37.785.
22. S.H. Vosko, L. Wilk, M. Nusair, Accurate spin-dependent electron liquid correlation energies for local spin density calculations: a critical analysis, Can. J. Phys. 58 (1980) 1200-1211. https://doi.org/10.1139/p80-159.
23. P.J. Stephens, F.J. Devlin, C.F. Chabalowski, M.J. Frisch, Ab Initio Calculations of Vibrational Absorption and Circular Dichroism Spectra Using Density Functional Force Fields, J. Phys. Chem. 98(45) (1994) 11623-11627. https://doi.org/10.1021/j100096a001.
24. R. Krishnan, J.S. Binkley, R. Seeger, J.A. People, Self-consistent molecular orbital methods. XX. A basis set for correlated wave functions, J. Chem. Phys. 72 (1980) 650. https://doi.org/10.1063/1.438955.
25. National Institute of Standards and Technology, Precomputed vibrational scaling factors. https://cccbdb.nist.gov/vibscalejust.asp, Release 22, May 2022.
26. M.P. Andersson, P. Uvdal, New Scale Factors for Harmonic Vibrational Frequencies Using the B3LYP Density Functional Method with the Triple-ζ Basis Set 6-311+G(d,p), J. Phys. Chem. A 109(12) (2005) 2937-2941. https://doi.org/10.1021/jp045733a.
27. C.H. Townes, A.L. Schawlow, Microwave Spectroscopy, Dover Publications, 2013.
28. H.W. Kroto, Molecular Rotation Spectra, Wiley, 1975.
29. R. Lindenmaier, N.K. Scharko, R.G. Tonkyn, K.T. Nguyen, S.D. Williams, T.J. Johnson, Improved assignments of the vibrational fundamental modes of *ortho*-, *meta*-, and *para*-xylene using gas- and liquid-phase infrared and Raman spectra combined with ab initio calculations: Quantitative gas-phase infrared spectra for detection, J. Mol. Struct. 1149 (2017) 332-351. https://doi.org/10.1016/j.molstruc.2017.07.053.
30. G.B. Lebron, T.L. Tan, Integrated Band Intensities of Ethylene ($^{12}C_2H_4$) by Fourier Transform Infrared Spectroscopy, Int. J. Spectrosc. (2012) 474639. https://doi.org/10.1155/2012/474639.
31. B.A. McGuire, P.B. Carroll, R.A. Loomis, I.A. Finneran, P.R. Jewell, A.J. Remijan, G.A.Blake, Discovery of the interstellar chiral molecular propylene oxide (CH_3CHCH_2O), Science 352(6292) (2016) 1449-1452. DOI: 10.1126/science.aae0328.
32. M.J. Wilhelm G.A. Petersson, J.M. Smith, D. Behrendt, J. Ma, L. Letendre, H.-L. Dai, UV Photolysis of Pyrazine and the Production of Hydrogen Isocyanide, J. Phys. Chem. A 122(46) (2018) 9001-9013. https://doi.org/10.1021/acs.jpca.8b09179.
33. C. Geron, R. Rasmussen, R.R. Arnts, A. Guenther, A review and synthesis of monoterpene speciation from forests in the United States, Atmos. Environ. 34 (2000) 1761-1781. https://doi.org/10.1016/S1352-2310(99)00364-7.
34. T.J. Johnson, P.M. Aker, N.K. Scharko, S.D. Williams, Quantitative infrared and near-infrared gas-phase spectra for pyridine: Absolute intensities and vibrational assignments, J. Quant. Spectrsoc. Radiat. Transf. 206 (2018) 355-366. https://doi.org/10.1016/j.jqsrt.2017.11.023.
35. L.T.M. Profeta, R.L. Sams, T.J. Johnson, S.D. Williams, Quantitative Infrared Intensity Studies of Vapor-Phase Glyoxal, Methylglyoxal, and 2,3,-Butanedione (Diacetyl) with Vibrational Assignments, J. Phys. Chem. A 115(35) (2011) 9886-9900. https://doi.org/10.1021/jp204532x.
36. S.D. Williams, T.J. Johnson, S.W. Sharpe, V. Yavelak, R.P. Oates, C.S. Brauer, Quantitative vapor-phase IR intensities and DFT computations to predict absolute IR spectra based on molecular structure: I. Alkanes, J. Quant. Spectrsoc. Radiat. Transf. 129 (2013) 298-307. https://doi.org/10.1016/j.jqsrt.2013.07.005.
37. M.J. Wilhelm, M. Nikow, L. Letendre, H.-L. Dai, Photodissociation of vinyl cyanide at 193 nm: Nascent product distributions of the molecular elimination channels, J. Chem. Phys. 130 (2009) 044307. https://doi.org/10.1063/1.3065986.

ACCEPTED MANUSCRIPT
AIP Advances
AIP Publishing
This is the author's peer reviewed, accepted manuscript. However, the online version of record will be different from this version once it has been copyedited and typeset.
PLEASE CITE THIS ARTICLE AS DOI: 10.1063/5.0155054

38. J.A. Devine, M.L. Wiechman, B. Laws, J.Chang, M.C. Babin, G. Balerdi, C. Xie, C.L. Malbon, W.C. Lineberger, D.R. Yarkony, R.W. Field, S.T. Gibson, J. Ma, H. Guo, D.M. Neumark, Encoding of vinylidene isomerization in its anion photoelectron spectrum, Science 358(6361) (2017) 336-339. DOI: 10.1126/science.aao1905.
39. M.J. Wilhelm, W. McNavage, R. Groller, H.-L. Dai, The $\nu_1 v_1$ CH stretching mode of the ketenyl (HCCO) radical, J. Chem. Phys. 128 (2008) 064313. https://doi.org/10.1063/1.2829400.
40. M.J. Wilhelm, W. McNavage, J.M. Smith, H.-L. Dai, The lowest quartet-state of the ketenyl (HCCO) radical: Collision-induced intersystem crossing and the v_2 vibrational mode, Chem. Phys. 244 (2013) 290-296. https://doi.org/10.1016/j.chemphys.2013.04.011.
41. M.J. Wilhelm, E. Martínez-Núñez, J. González-Vázquez, S.A. Vázquez, J.M. Smith, H.-L. Dai, Is Photolytic Production a Viable Source of HCN and HNC in Astrophysical Environments? A Laboratory-based Feasibility Study of Methyl Cyanoformate, ApJ, 849(15) (2017) 1-12. DOI 10.3847/1538-4357/aa8ea7.
42. J.M. Smith, M. Nikow, J. Ma, M.J. Wilhelm, T.-C. Han, A.R. Sharma, J.M. Bowman, H.-L. Dai, Chemical Activation through Super Energy Transfer Collisions, J. Am. Chem. Soc. 136(5) (2014) 1682-1685. https://doi.org/10.1021/ja4126966.
43. E.B. Wilson, J.C. Decius, P.C. Cross, Molecular Vibrations: The Theory of Infrared and Raman Vibrational Spectra, Dover Publications, 1980.

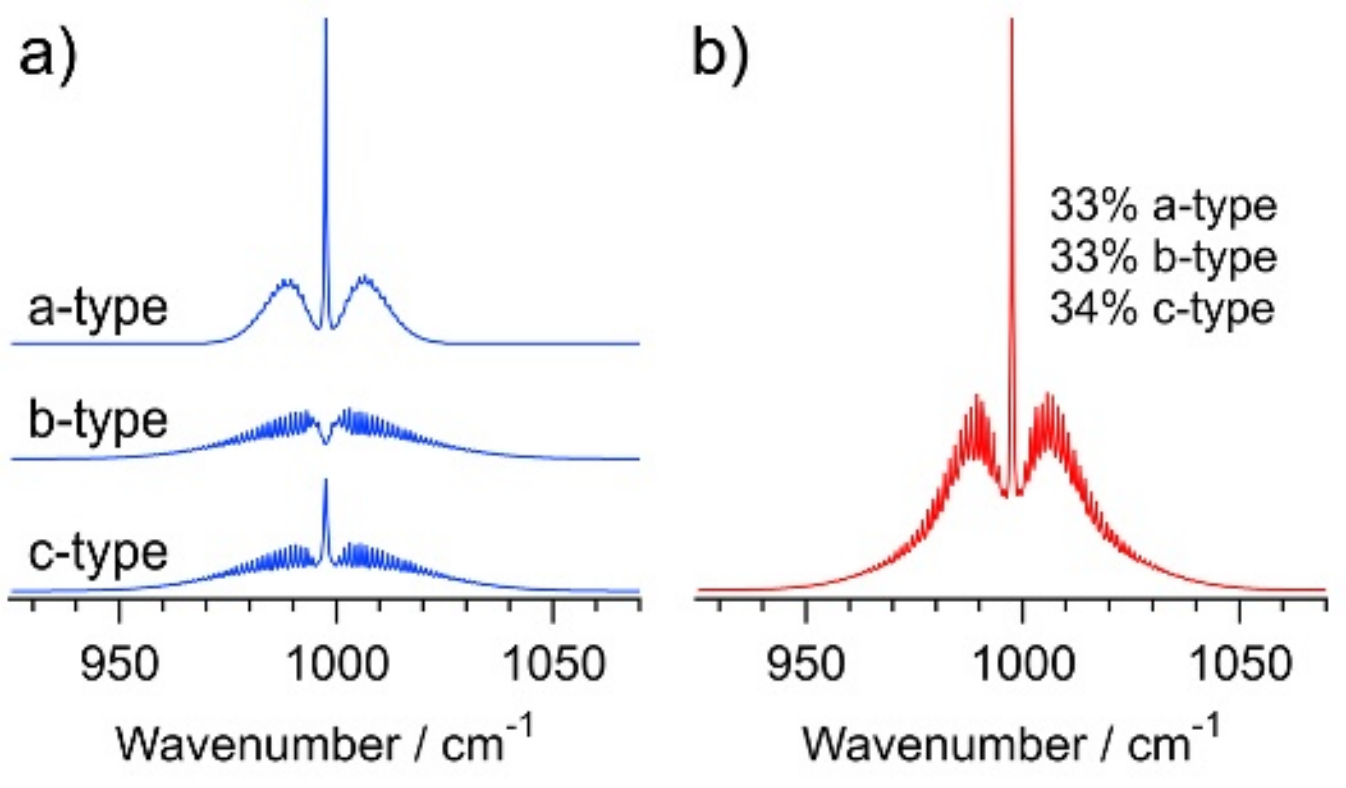
a)
a-type
b-type
c-type
950
1000
1050
Wavenumber / cm-1
b)
33% a-type
33% b-type
34% c-type
950
1000
1050
Wavenumber / cm-1

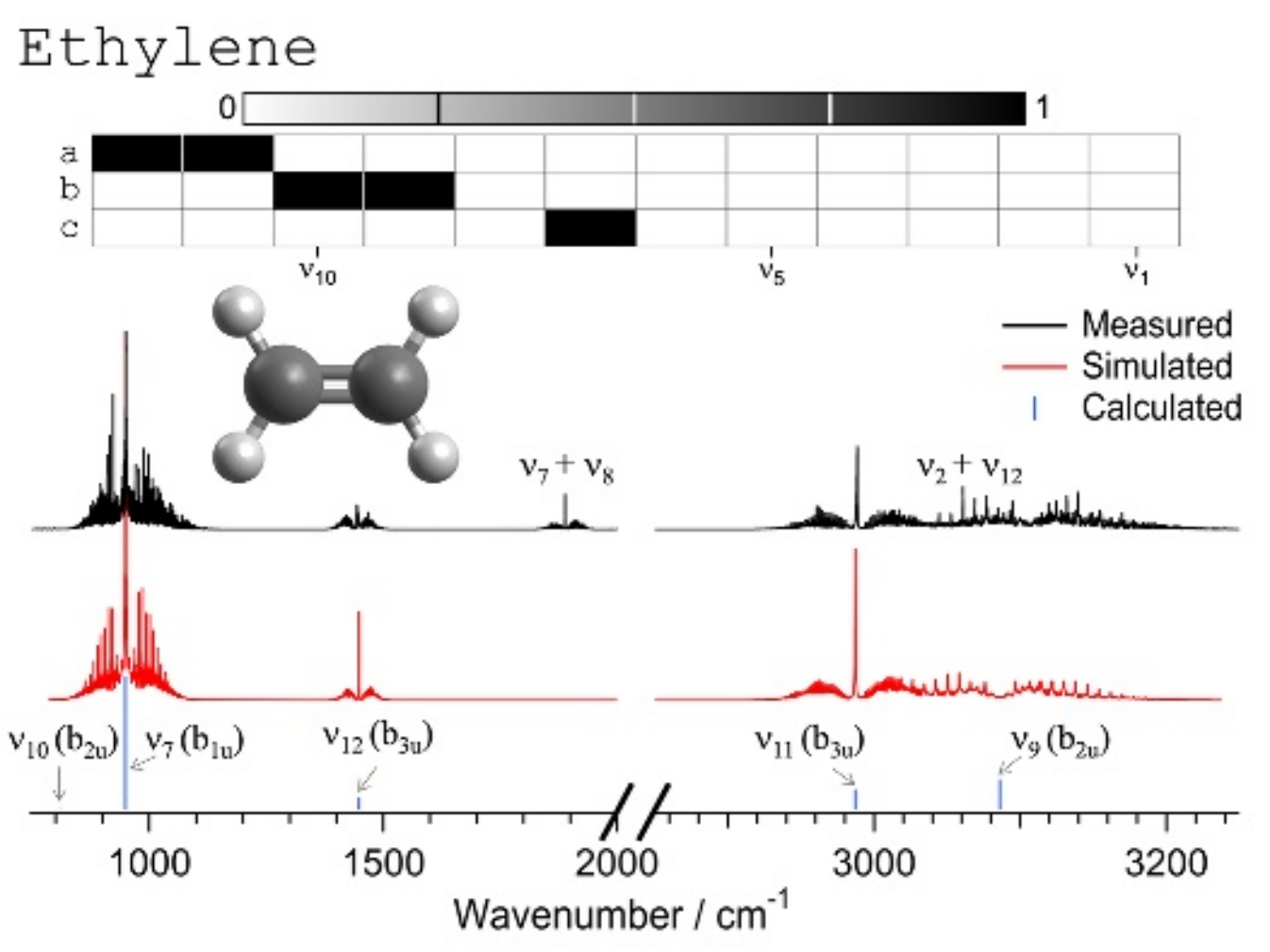
Ethylene
0
1
a
b
c
ν_{10}
ν_5
ν_1
Measured
Simulated
Calculated
$\nu_7 + \nu_8$
$\nu_2 + \nu_{12}$
ν_{10} (b_{2u})
ν_7 (b_{1u})
ν_{12} (b_{3u})
ν_{11} (b_{3u})
ν_9 (b_{2u})
1000
1500
2000
3000
3200
Wavenumber / cm^{-1}

Propylene Oxide

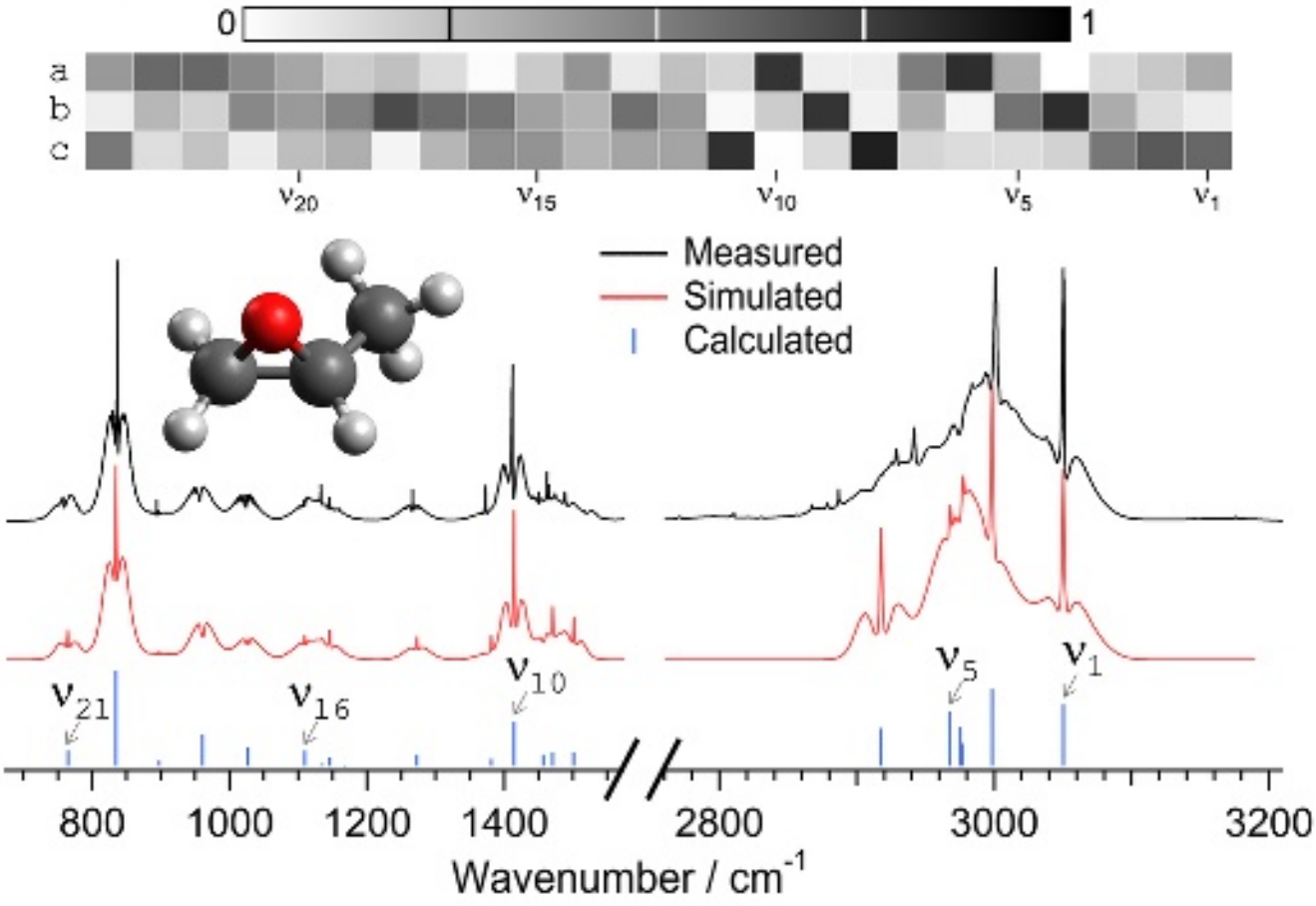

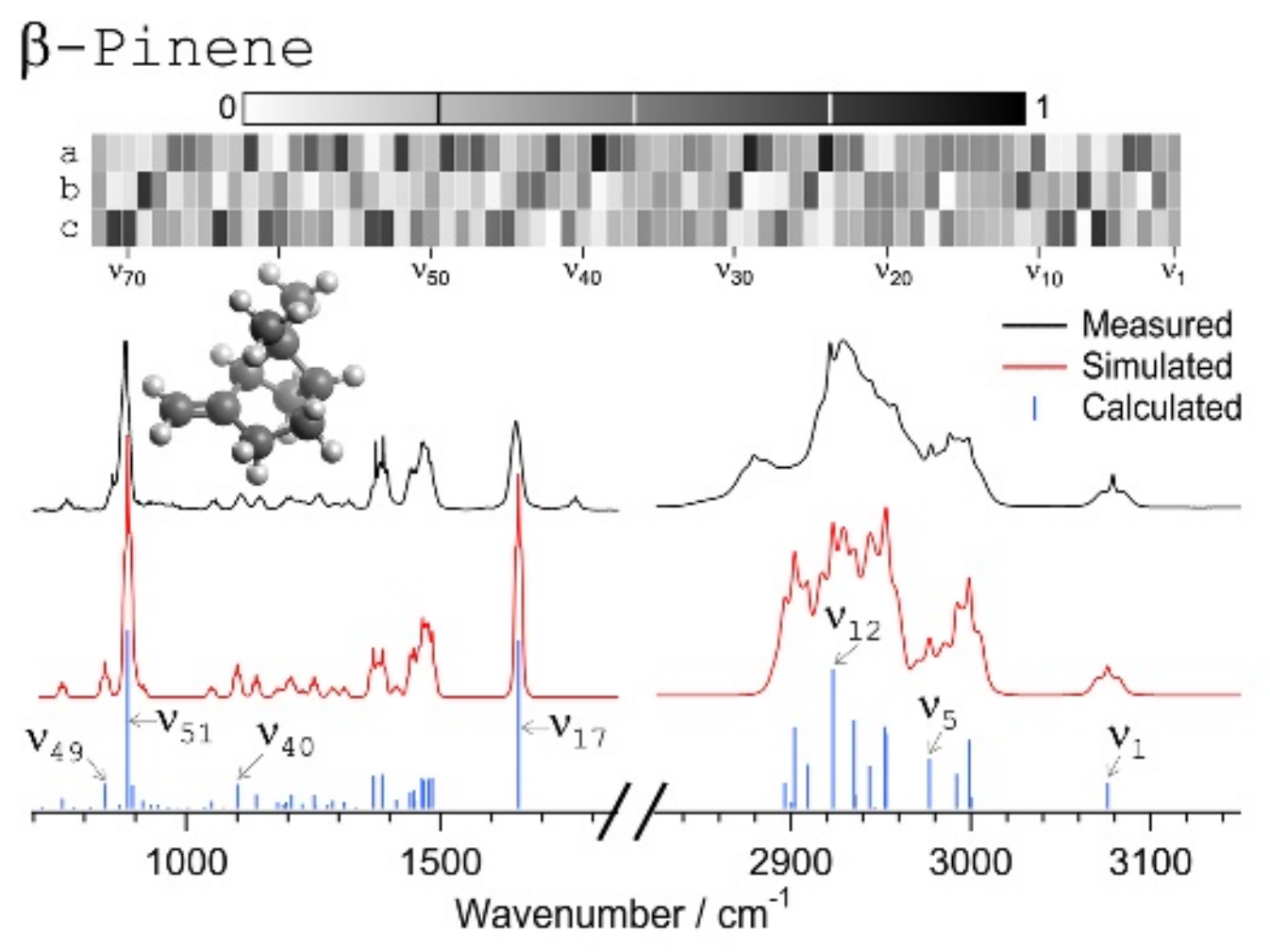
β-Pinene
0
1
a
b
c
ν70
ν50
ν40
ν30
ν20
ν10
ν1
Measured
Simulated
Calculated
ν49
ν51
ν40
ν17
ν12
ν5
ν1
1000
1500
2900
3000
3100
Wavenumber / cm-1

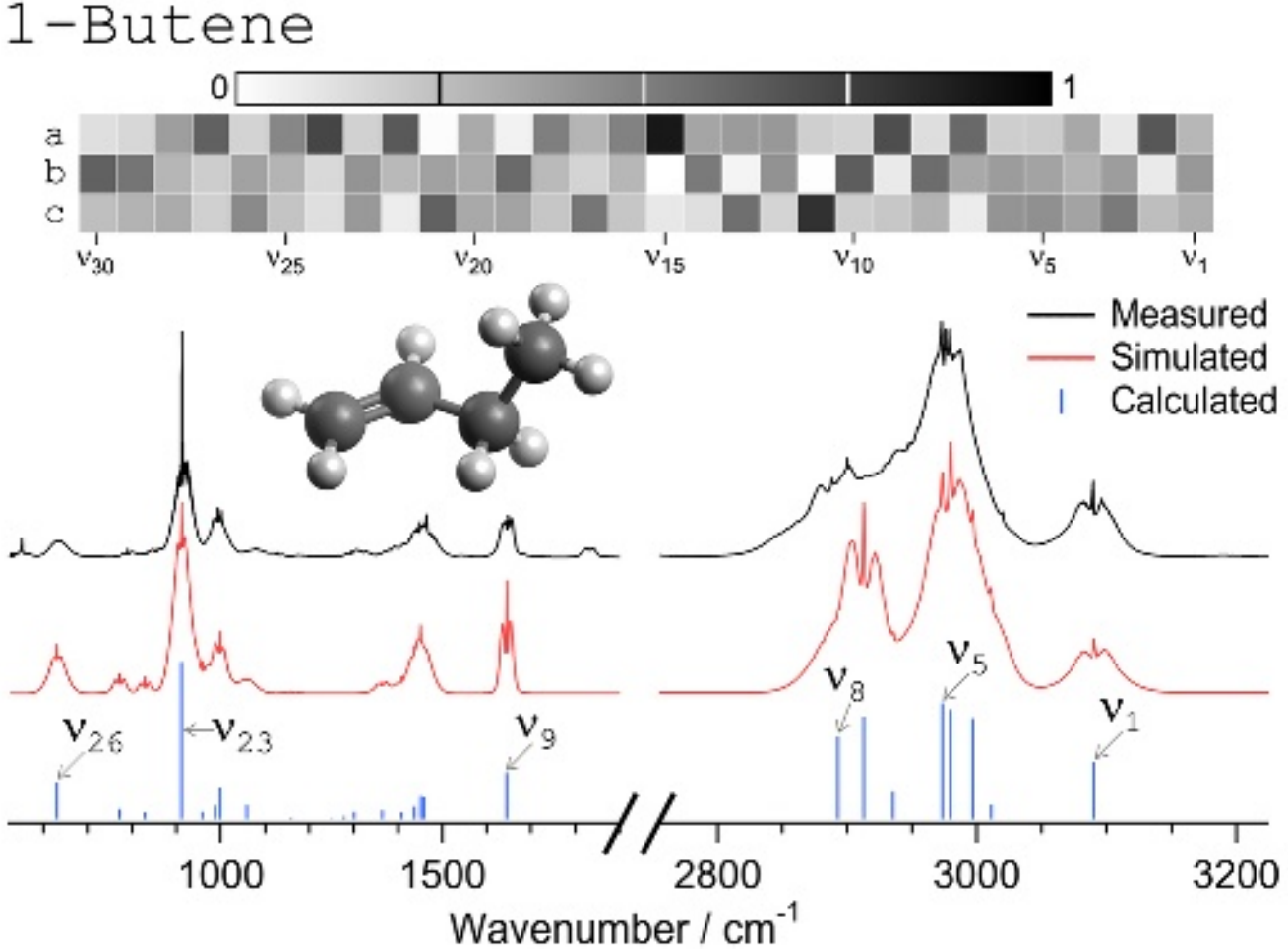
1-Butene
0
1
a
b
c
ν30
ν25
ν20
ν15
ν10
ν5
ν1
Measured
Simulated
Calculated
ν26
ν23
ν9
ν8
ν5
ν1
1000
1500
2800
3000
3200
Wavenumber / cm-1

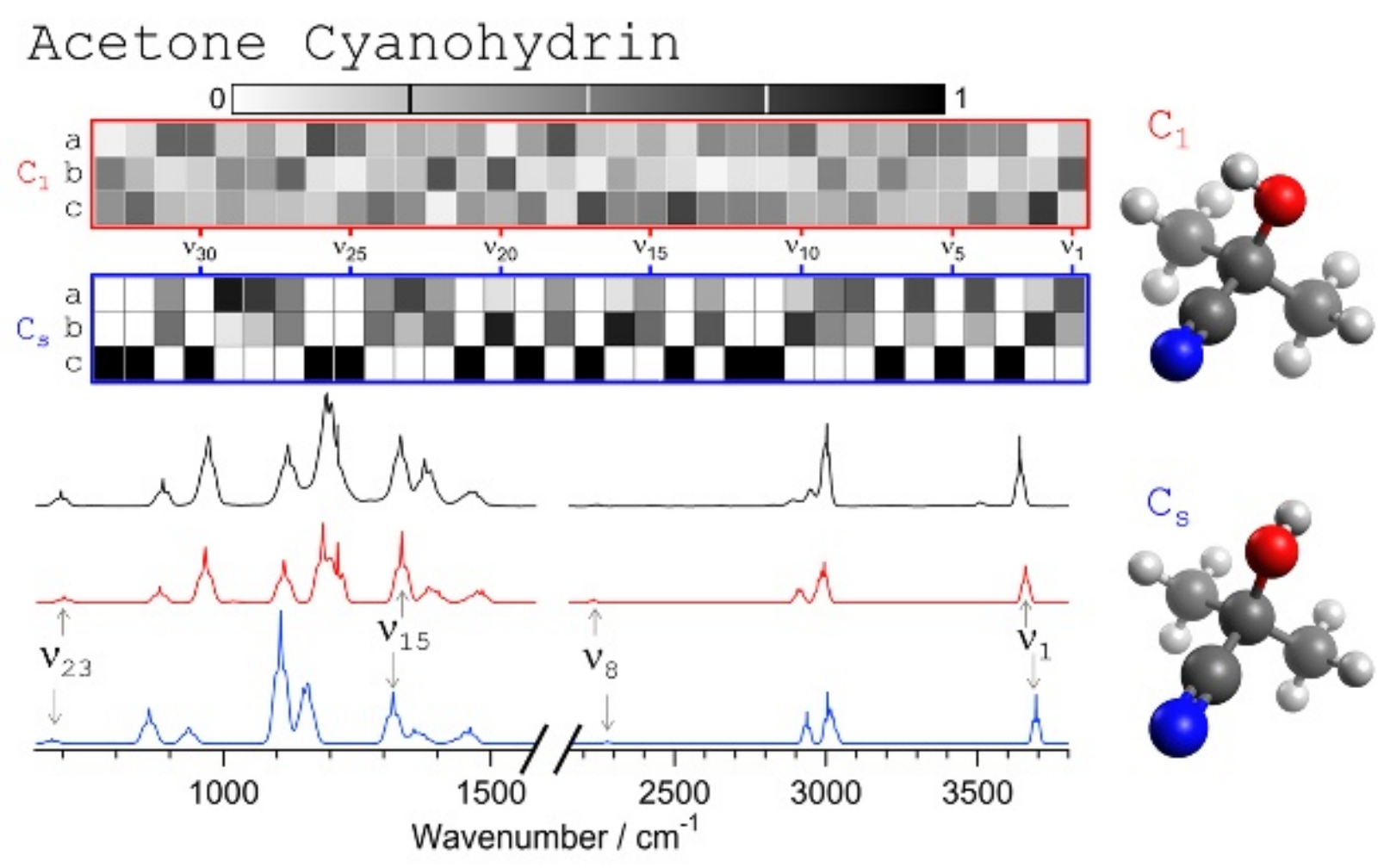
Acetone Cyanohydrin
0
1
C1
a
b
c
ν30
ν25
ν20
ν15
ν10
ν5
ν1
Cs
a
b
c
C1
Cs
ν23
ν15
ν8
ν1
1000
1500
2500
3000
3500
Wavenumber / cm-1